PERGAMON

Carbon 40 (2002) 1863–1872

CARBON

Adsorption on carbonaceous surfaces: cost-effective computational strategies for quantum chemistry studies of aromatic systems

Alejandro Montoya[a], Fanor Mondragón[a], Thanh N. Truong[b,*]

[a]*Department of Chemistry, University of Antioquia, Medellin, Colombia A.A 1226*
[b]*Henry Eyring Center for Theoretical Chemistry, Department of Chemistry, University of Utah, 315 South 1400 East, rm 2020, Salt Lake City, UT 84112, USA*

Received 12 May 2001; accepted 23 November 2001

Abstract

We present a systematic analysis of the accuracy and efficiency of several computational quantum chemistry models for studying reactions involving aromatic systems. In particular, we have examined different multi-layer ONIOM models in which the whole system is divided into subsystems that can be treated at different levels of theory. The carbonaceous surface is modeled by a graphene layer that has unsaturated carbon atoms to represent active sites and has different shapes to simulate the local environment of the active sites of a carbonized material. We emphasized the model performance in predicting geometrical parameters, interaction energies and infrared spectra of carbon–oxygen complexes. We found that any attempt to partition the graphene layer into subsystems for employing different levels of theory yields considerable errors. However, it is possible to obtain reasonable accuracy by using the same level of theory for the whole system at different basis sets. This computational strategy can predict accurate geometrical parameters, interaction energies and infrared spectra of common oxygen complexes at lower computational cost.

Keywords: A. Char, Carbon nanotubes; C. Computational chemistry; D. Adsorption properties, Surface oxygen complexes

1. Introduction

Carbon is an important industrial element that exists in different sp^2-network assemblies, such as graphite, fullerenes, single-shell nanotubes and char structures. Unlike the others, which have regular structures, char surfaces obtained from coal have random orientations and translations of sp^2-bound subunits. Properties of these materials are highly dependent on the network organization of the carbon atoms. Thus, success in most industrial applications depends crucially on the atomic level understanding of the chemical reactions occurring on the carbonaceous surface. There has been a long history in research on the carbonaceous materials, especially on the combustion and gasification of char using different experimental techniques. However, the drastic experimental conditions at which the aromatic network is decomposed make it difficult to study the detailed mechanism of reactions at the molecular level. Therefore, to obtain such information, state-of-the-art quantum chemistry methods are viable alternatives and have been recently applied to study the mechanism of reactions that take place in gasification and combustion [1–4].

Chemical reactions on these carbonaceous surfaces take place mainly on the edge of the graphene layer, especially on single-shell nanotubes [5–8] and char surfaces [9,10] where some carbon atoms at the edge of the aromatic unit remain unsaturated. Experimental techniques such as X-ray diffraction, electrical resistivity, and electron microscopy have been used to elucidate physical structures of these materials [11–14]. In general, the sp^2-carbon network is conceived as a macrostructure that contains five- and six-member rings in armchair and zigzag shapes. On char surfaces, aromatic units of three to seven six-carbon rings

*Corresponding author. Tel.: +1-801-581-7272; fax: +1-801-581-4353.
E-mail address: truong@chem.utah.edu (T.N. Truong).

0008-6223/02/$ – see front matter
PII: S0008-6223(02)00035-0

[15] are bonded together in random orientation to form a three-dimensional network. The unsaturated carbon atoms on the edge of the aromatic unit are the active sites in the chemisorption of gasifying agents [9]. Also, the open part of a single-shell nanotube structure contains unsaturated carbon atoms and dangling bonds that are the active sites for growing the carbon network [5].

To model chemical reactions in gasification, combustion and single-shell nanotubes where chemical bonds are broken or formed, one requires accurate quantum chemistry methods. The computational demand, however, has limited the physical models of char to a single-layer graphene consisting of four to nine six-member rings where some carbon atoms are unsaturated to simulate the active sites. Previous theoretical studies have employed both Hartree–Fock (HF) and density functional theory (DFT) methods to study these models [1,16,17].

Due to the large number of possible reactions occurring at the carbon surface, it is still computationally quite demanding to accurately model reactions on different aromatic units with three to seven member rings. Thus, determining a more cost-effective computational strategy is particularly important for future studies of the mechanism of coal gasification or formation of single-wall nanotubes. Since only the active sites are directly involved in reactions with gaseous species, can we treat the remaining region of the carbon surface using a lower level of theory without losing much accuracy in the calculated chemical properties? This is the main question to be addressed in this study. The ONIOM approach developed by Morokuma and co-workers is well suited for investigating this problem [18,19]. In this approach, the real system is divided into several subsystems that can be treated at different levels of theory. The small region that is most sensitive and critical to the calculated properties can be treated at a very accurate level of theory. The spectator regions, according to their relative importance, can be modeled at different lower levels of theory. The goal of this study is to examine the accuracy of this approach and to establish a cost-effective computational strategy for modeling reactions on the carbonaceous solid surface. A previous study has found that the ONIOM approach, particularly the integrated molecular orbital+molecular orbital (IMOMO) method, can accurately predict chemical properties of reactions involving aliphatic hydrocarbons [20], although larger errors were observed for breaking the C=C bond completely due to delocalization/conjugation of the molecular system studied [21]. For this study, due to resonance structures in aromatic systems, it is difficult to select an appropriate model system. Several different partition schemes for doing so are examined.

2. Computational details

2.1. Physical models

Two carbon models as shown in Fig. 1 were selected. They represent finite carbon models in armchair and zigzag shape as can be found in a carbonized surface. The boundary conditions are capped with hydrogen atoms and several unsaturated carbon atoms are used to represent the active sites. Because we want to compare different theoretical levels, these models are sufficient for the purpose of this study.

Since not all CC bonds or CCC angles are the same due to the finite graphene layer, Fig. 1 shows the unique bonds and angles by their topology. The unique bonds are defined by the nature of the carbon atom type. For instance, unsaturated carbon atoms, namely ‘a’, are the carbon atoms without hydrogen atom termination and are located at two-edge vertices. The inactive exposed carbons, namely ‘ie’, are the carbon atoms located at three-edge vertices. The inactive buried carbons, namely ‘ib’, are the carbon atoms also located at three-edge vertices but they are differentiated from the ‘ie’ carbons in that they are not exposed to the plane of adsorption of the gas molecule. The word ‘active’ or ‘inactive’ refers to the unsaturated or saturated carbon atom. Active carbons are the active sites of the caronaceous surface. The unique bond lengths and

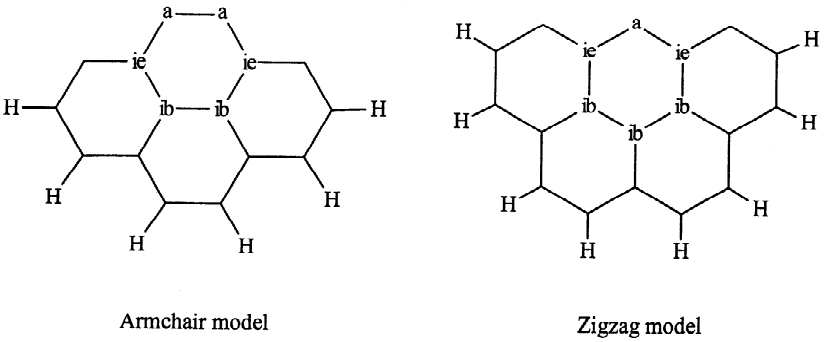

Fig. 1. Selected models of a carbonaceous structure. Letters denote the nature of the selected carbon atoms. (a) Active site; (ie) inactive exposed site; (ib) inactive buried site.

angles represented in Fig. 1 were selected in order to discuss the performance of different theoretical methods.

2.2. Theoretical method

In this study, electronic ground states were used for all molecular systems. These ground states were determined from single-point energy calculations at the B3LYP/6-31G(d) level of theory for several low-lying electronic states and the lowest energy state was selected for each molecular system. We used the B3LYP/6-31G(d) as the reference level since it can provide accurate potential energy surface information as shown in our previous study [22]. In particular, the B3LYP [23] functional usually produces fairly accurate bond energies and accurate geometrical parameters. The 6-31G(d) basis set was the largest basis set considered here. It includes a set of 'd' functions on the carbon atoms to allow polarization on the carbon orbitals during adsorption/desorption of gaseous species. From this reference point, we examine the accuracy of several less computationally demanding (also less accurate) methods, namely the Hartree–Fock (HF) and the semiempirical AM1 methods with several smaller basis sets, namely the STO-3G, 3-21G and MIDI! basis sets. MIDI! is the minimal basis set with a set of d polarization functions [24]. The ab-initio Hartree–Fock level was used because it has been previously used for estimating geometries of graphene models [16]. Semiempirical calculation at the AM1 level was also included due to its simplicity and low computational cost to model larger carbonaceous model structures [25].

In addition to the traditional electronic structure methods mentioned above, we also examined several schemes using the multi-layer ONIOM approach. The molecular structures were divided into real and model systems as shown in Fig. 2. In all cases, the real system corresponds to the full molecular structure; it was studied with a low level of theory. A small part of the real system was studied with a higher level of theory and it represents the model system. In Fig. 2a the model system corresponds to the first row of carbon atoms, which was studied with the highest level of theory to describe the electron reorganization of the active sites during the interaction with a gas. Notice that all active sites of the real system belong to the small system and they are treated at a high level of theory. In Fig. 2b the model system was selected in a different way. In this case, it corresponds to the central six-member ring of the real system. Notice that not all active sites of the real system

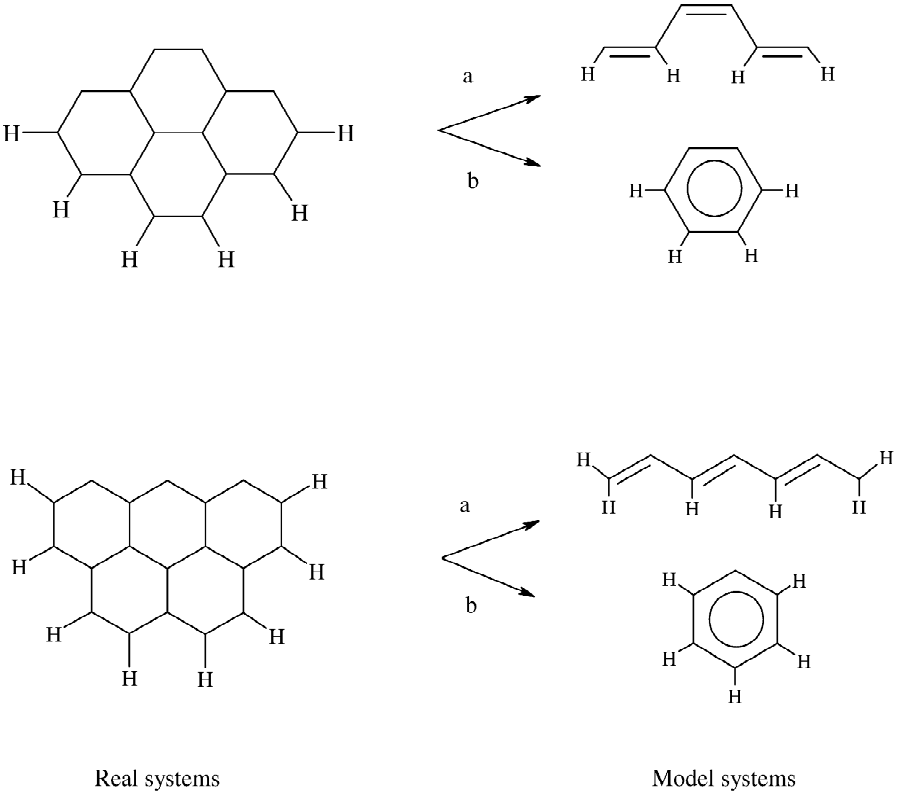

Fig. 2. Schematic representation of the different systems in the multiple-layer ONIOM model for the armchair and zigzag carbonaceous models.

Table 1
Selected optimized geometrical parameters of the unique bonds and angles for the $C_{16}H_6$ armchair model at different level of theory. Bond lengths in pm and bond angles in degrees

Parameter	B3LYP				HF		AM1
	6-31G(d)	MIDI!	3-21G	STO-3G	3-21G	6-31G(d)	
a–a	123.33	0.06	0.04	0.77	8.76	−3.00	8.16
a–ie	141.79	−0.02	0.16	2.57	0.00	1.50	−2.30
ie–ib	146.54	0.37	0.78	1.75	−1.57	−2.16	−0.79
ib–ib	143.80	−0.24	0.05	2.62	−0.56	2.82	−0.72
<a–a–ie	128.18	0.00	0.09	0.28	−4.28	0.27	−2.86
<a–ie–ib	109.88	0.03	−0.04	−0.51	5.27	−0.23	3.61
<ie–ib–ib	121.94	−0.06	−0.09	0.16	−1.21	−0.11	−0.87

are studied at a high level of theory. Instead, the six-member ring that interacts with a gas is studied at a high level of theory. Partitioning the carbonaceous model into real and model systems yields the two-layer ONIOM method. However, since hydrogens in the real system are the boundary-capped atoms of the molecular models, they can be studied at a lower level of theory in a three-layer ONIOM method. The nomenclature of the two-layer ONIOM method will be given in the following order: 'Model system: Real system'. Similarly, 'Model system: Real system: capped atoms' is for the three-layer ONIOM method.

The first ONIOM model selected was named OL2-BH(L) (O, ONIOM; L2, two-layer ONIOM method; B, B3LYP; H, Hartree–Fock; (L), Linear chain in the active region). It corresponds to the B3LYP/6-31G(d):HF/3-21G level of theory. The second ONIOM model was named OL3-B(L). It corresponds to B3LYP/6-31G(d):B3LYP/3-21G:B3LYP/STO-3G. This level uses the B3LYP functional for the whole system but uses three different basis sets for different regions. The third ONIOM model was named OL2-BA(L). It corresponds to the B3LYP/6-31G(d):AM1 level of theory and the model system is shown in Fig. 2a. The final ONIOM model, OL2-BA(R), corresponds to the B3LYP/6-31G(d):AM1 level of theory where the model system is the central six-member ring as shown in Fig. 2b. In all cases, including the ONIOM methods, unrestricted wave functions were used in all open-shell cases. All calculations were performed using the GAUSSIAN 98 program [26].

3. Results and discussion

3.1. Geometrical parameters

3.1.1. Carbonaceous models

The geometrical parameters of the unique bonds and angles predicted by the different methods are shown in Tables 1 and 2. Unfortunately, there are no experimental data for the geometry of carbonaceous surfaces that can differentiate between the a–a and a–i bonds. Thus, we rely on the geometry obtained at the highest theoretical level as the reference point. Table 1 presents the data for the $C_{16}H_6$ armchair model and Table 2 presents the data for the $C_{19}H_8$ zigzag model. In all cases, optimizations of both models yield planar geometries. Bond lengths and angles obtained from the B3LYP/6-31G(d) level are shown in column 2. The other columns show the differences with respect to the geometrical parameters at the B3LYP/6-31G(d) level. For instance, the a–a bond length in Table 1 at the B3LYP/MIDI! level is 0.06 pm longer than that at the B3LYP/6-31G(d) level.

By arranging them according to the bond type, we can see some trends; for instance, the active–active bonds are shorter than the active–inactive bonds which in turn are

Table 2
Selected optimized geometrical parameters of the unique bonds and angles for the $C_{19}H_8$ zigzag model at different level of theory. Bond lengths in pm and bond angle in degrees

Parameter	B3LYP				HF		AM1
	6-31G(d)	MIDI!	3-21G	STO-3G	3-21G	6-31G(d)	
a–ie	139.37	−0.11	0.09	2.93	0.58	0.58	−1.50
ie–ib	145.38	0.01	0.48	1.62	−0.71	−0.71	0.14
ib–ib	142.70	−0.19	0.08	2.10	−0.42	0.02	−0.08
<a–ie–ib	116.82	0.04	0.18	0.58	0.37	0.55	−1.40
<ie–ib–ib	119.71	−1.06	0.04	0.09	0.09	0.09	−0.14
<ib–ib–ib	120.75	0.06	0.01	−0.15	−0.16	−5.59	0.30
<ie–a–ie	126.18	−0.10	−0.26	1.68	−1.12	−0.32	2.76

Table 3
Optimized geometrical parameters of the unique bonds and angles at different ONIOM levels for the armchair model. Bond lengths in pm and bond angles in degrees

Parameter	B3LYP/6-31G(d)	OL3-B(L)	OL2-BH(L)	OL2-BA(L)	OL2-BA(R)
a–a	123.33	0.02	0.01	1.24	13.66
a–ie	141.77	−0.03	−0.21	0.97	−0.01
ie–ib	146.55	−0.02	0.22	−1.03	−0.44
ib–ib	143.80	0.06	1.42	0.15	0.06
>a–a–ie	128.18	0.01	0.02	−2.30	−5.50
>a–ie–ib	109.88	−0.02	0.36	0.82	7.48
>ie–ib–ib	121.94	0.00	−0.39	0.16	−1.85

shorter than the inactive–inactive bonds. This indicates that there are significant interactions between the unpaired electrons in the two in-plane sigma orbitals of the neighboring active sites. The angle is also opened up in the armchair model to facilitate this type of bonding. The parameters predicted at the B3LYP using the 6-31G(d), MIDI! and 3-21G basis set for the armchair and the zigzag models are almost the same. A small deviation is found at the STO-3G basis set. This indicates that the geometrical parameters are not sensitive to the basis sets beyond the minimal one. The geometrical parameters at the HF levels have considerable deviations from our reference point, in particular for the a–a bond in the armchair model. These large differences between the B3LYP and HF geometries may be due to the lack of electron correlation in the HF wavefunctions. Thus, electron correlation is important for geometrical parameters. Large deviations in the AM1 results were also found for the active–active bond, although the deviations were smaller for other geometrical parameters. These results suggest that the B3LYP/6-31G(d) level should be used for the active part of the model, the 3-21G basis set for the remaining carbon atoms and B3LYP/STO-3G or AM1 for the boundary hydrogen atoms.

The geometrical parameters of the unique bonds and angles predicted using the four ONIOM methods are shown in Tables 3 and 4. All ONIOM methods predict planar geometries for the carbonaceous structures, which is consistent with the B3LYP results. The OL3-B(L), OL2-BH(L) and OL2-BA(L) levels predicted almost the same bond lengths and bond angles as those obtained from the B3LYP/6-31G(d) calculations. The percentages of deviation are not more than 1.0% in the bond lengths and 1.5% in the bond angles. However, the best agreement is obtained from the OL3-B(L) model. The geometrical results predicted with the OL2-BA(L) level are much better than those from the HF/3-21G and B3LYP/STO-3G methods. The geometrical parameters from the OL2-BA(R) model are not as good as those obtained with the other ONIOM methods. Considerable deviations of 11 and 7% in the a–a bond length and a–ie–ib angle, respectively, for the armchair model were observed. This suggests that the neighboring unsaturated carbons have a strong effect on the overall geometry of the complete molecular model and they should be studied at the highest level of theory.

3.1.2. Carbon–oxygen complexes

We used the interaction of carbon monoxide and atomic oxygen with the carbonaceous models to test the accuracy of different ONIOM methods. For carbon monoxide, although there are different possible interaction configurations, we restricted ourselves to examine only the formation of a carbonyl group as shown in Fig. 3. Similarly, for atomic oxygen, we restricted our study to the formation of a semiquinone group.

Several important optimized geometrical parameters of

Table 4
Optimized geometrical parameters of the unique bonds and angles at different ONIOM levels for the zigzag model. Bond lengths in pm and bond angles in degrees

Parameter	B3LYP/6-31G(d)	OL3-B(L)	OL2-BH(L)	OL2-BA(L)	OL2-BA(R)
a–ie	139.37	0.14	0.49	0.81	1.44
ie–ib	145.38	0.63	0.91	−1.33	2.68
ib–ib	142.70	0.09	−0.10	0.09	−1.50
<a–ie–ib	116.82	0.03	0.17	−0.72	0.92
<ie–ib–ib	119.71	0.00	0.05	0.25	0.67
<ib–ib–ib	120.75	0.02	0.07	0.23	−0.38
<ie–a–ie	126.18	−0.10	−0.52	0.70	−2.80

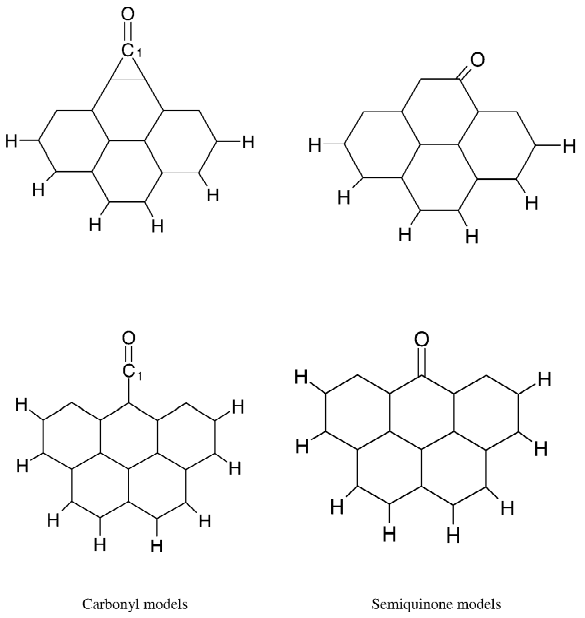

Fig. 3. Carbon–oxygen surface complexes formed after interaction with carbon monoxide and atomic oxygen. The carbon atom of the carbonyl group is numbered to facilitate the discussion.

the carbon–oxygen complexes are shown in Table 5. Optimized B3LYP/6-31G(d) bond lengths are shown in column 2. The other columns show the differences in the geometrical parameters similar to the previous tables. First of all, it was found at the B3LYP/631-G(d) level that the bond length of the carbonyl C–O group varies depending on the shape of the local active site, while the bond length of the semiquinone C–O group is less affected. Models in zigzag have the shortest C–O bond length. Compared to the experimental value of 112.8 pm for an isolated carbon monoxide [27], the carbonyl C–O bond in the zigzag model is the least affected one upon interaction. Since CO has a three-center bond to the armchair model, one can expect the corresponding C–O bond length to be longer than that of the zigzag model, which has the typical two-center bond with the C=O group. It was found that all ONIOM methods predict the surface carbonyl and semiquinone complexes to be planar, consistent with the full B3LYP/6-31G(d) results. Furthermore, all ONIOM methods predict acceptable geometrical parameters. However, similar to the geometrical parameters of the purely carbonaceous structures, the OL3-B(L) method gives the best performance on carbon–oxygen complexes and keeps the same trend on the C–O bond lengths at different active sites as was found with our reference point. The OL2-BA(L) method predicts much better results than the OL2-BH(L) and OL2-BA(R) methods.

3.2. Energetic features

The interaction energies of carbon monoxide and atomic oxygen in the armchair and the zigzag models at different levels of theory were obtained with special emphasis on the performance of the ONIOM methods. Because we want to compare the performance of different theoretical models, the absolute interaction energy is not important at this point. Thus, the interaction energy obtained at different theoretical levels is compared with that obtained at the B3LYP/6-31G(d) level chosen as the reference point. Table 6 shows the interaction energy at different levels of theory, namely the B3LYP/6-31G(d), ONIOM methods, HF/3-21G, B3LYP/6-31G(d)//HF/3-21G, and OL3-B(L)//B3LYP/STO-3G. The last two levels of theory calculate the interaction energy from single-point energy calculations at B3LYP/6-31G(d) and OL3-B(L) levels using the optimized HF/3-21G and B3LYP/STO-3G structures, respectively.

The interaction energy of atomic oxygen at the B3LYP/6-31G(d) level is approximately three times that of a CO

Table 5
Optimized geometrical parameters of selected carbon–oxygen complexes. Bond lengths are in pm

	Level of theory				
	B3LYP/6-31G(d)	OL3-B(L)	OL2-BA(L)	OL2-BH(L)	OL2-BA(R)
Armchair semiquinone					
C–O	123.48	−0.48	−0.03	2.87	0.40
Armchair carbonyl					
C–O	120.45	−0.02	−0.30	−0.12	−4.27
$C–C_1$	144.16	−0.05	0.53	0.08	5.82
Zigzag semiquinone					
C–O	122.54	0.31	1.20	−8.73	2.93
Zigzag carbonyl					
C–O	116.64	−0.07	1.02	1.24	3.51
$C–C_1$	133.53	0.23	5.15	−2.46	−2.50

Table 6
Interaction energy (in kcal/mol) of carbon monoxide and atomic oxygen in armchair and zigzag carbon models at different levels of theory[a]

Method	Armchair		Zigzag	
	CO	O	CO	O
B3LYP/6-31G(d)	−38.1	−111.1	−54.6	−161.7
OL3-B(L)	−38.8	−115.8	−56.2	−166.6
% dev	1.8	4.2	2.9	3.0
OL2-BH(L)	−38.7	−121.0	−42.4	−130.2
% dev	1.6	8.9	22.3	19.4
OL2-BA(L)	−37.5	−104.3	−51.2	−128.9
% dev	1.6	6.1	6.2	20.3
OL2-BA(R)	−63.7	−117.1	−48.1	−190.6
% dev	67.2	5.4	11.9	17.8
HF/3-21G	+25.2	−39.7	+25.9	−25.2
% dev	166.1	64.3	147.4	84.4
B3LYP/6-31G(d)// HF/3-21G	−38.9	−105.2	−53.1	−160.0
% dev	2.1	5.3	2.7	1.1
OL3-B(L)//B3LYP/ STO-3G	−35.8	−99.0	−54.2	−163.9
% dev	6.0	14.5	3.6	1.6

[a] % dev is relative to the B3LYP/6-31G(d) level.

molecule. The interaction energy for the armchair model is lower than for the zigzag model. The OL3-B(L) method predicts interaction energies with a deviation of less than 3%. The OL2-BH(L) method predicts fairly good results with a maximum deviation of 22% in the interaction energy in the zigzag model. Although the OL2-BA(L) method has a maximum deviation of 20% in the atomic oxygen interaction, it predicts much better energetic results than the OL2-BH(L) and the OL2-BA(R) methods. Contrary to the geometrical parameter results discussed earlier, all of the two-layer ONIOM methods yield large errors in the interaction energy of carbonaceous models with oxygen. These results indicate that partitioning a highly conjugated or aromatic system into different systems for treating them at different levels of theory would disrupt the delocalization effects of the π-bond network. Consequently, inaccurate interaction energies are predicted for the interaction of oxygen with the carbonaceous models. However, the three-layer OL3-B(L) ONIOM method (i.e. a small basis set for the boundary conditions, a large basis set for the model system and a medium basis set for the remaining carbon atoms at the B3LYP level) is able to give accurate interaction energies.

Although some of the ONIOM methods deviate from our reference point, they predict an exothermic interaction in all cases. A different trend is found at the HF/3-21G level. The interaction energy of atomic oxygen has a large deviation and the interaction energy of CO is predicted to be an endothermic process. The large deviation in the interaction energy of the HF level can be due to electron correlation effects and to the spin contamination on the single determinant HF wavefunction of char models as was discussed elsewhere [28]. Thus, we discard this level of theory for energetic prediction in subsequent discussions. For comparison purposes, Table 6 also shows results from the traditional approach, namely single-point energy calculations at a high level of theory using optimized structures at a lower level of theory. It is seen that the B3LYP/6-31G(d)//HF/3-21G and OL3-B(L)/B3LYP/STO-3G levels have a small interaction energy deviation. However, as pointed out in the previous section, lower levels of theory tend to predict erroneous geometrical parameters and extra care should be taken for transition states where electron correlation is important and spin contamination is often large.

3.3. Frequency calculations

Now we consider the calculated IR spectra of carbon–oxygen complexes. Three different levels of theory were selected, namely B3LYP/6-31G(d) as the reference point, OL3-B(L) because it is the ONIOM method that gives accurate geometries and interaction energies, and OL2-BA(L) for its fairly good performance at a low computational cost. Figs. 4 and 5 show the predicted IR spectra for the semiquinone and carbonyl models in zigzag and armchair structures, respectively.

B3LYP frequencies in Fig. 4a at 1613, 1650, and 1741 cm^{-1} are due to the >C=O stretching in the semiquinone group. Frequencies over 3000 cm^{-1} are the >C–H stretching, and frequencies between 1400 and 1600 cm^{-1} are due to the >C=C< stretching bonds. The most intense frequency is obtained at 1741 cm^{-1} for the >C=O stretching. The OL3-B(L) IR spectrum in Fig. 4b resembles very well that obtained at the B3LYP/6-31G(d) level. In particular, it has >C=O stretching frequencies at 1602, 1651, and 1740 cm^{-1}, which are very close to those of the B3LYP/6-31G(d) spectrum. Frequencies over 3000 cm^{-1} are the >C–H stretching and those between 1400 and 1600 cm^{-1} are due to the >C=C< bonds. The intensity patterns and the frequency values resemble those obtained at the B3LYP/6-31G(d) level. Fig. 4c shows the IR spectrum obtained at the OL2-BA(L) ONIOM level. It was found that frequencies at 1584 and 1677 cm^{-1} are due to the >C=O stretching in the semiquinone group. The frequency values deviate at most 65 cm^{-1} from the frequency values obtained at the B3LYP/6-31G(d) level of theory. The >C=O stretching mode does not correspond to the highest intensity and the general pattern of the spectrum is different from that obtained at the other two levels of theory.

Fig. 5a shows carbonyl –C=O stretching at 1963 cm^{-1} at the B3LYP/6-31G(d) level; frequencies over 3000 cm^{-1} are due to the C–H stretching and those between 1400 and 1600 cm^{-1} to the >C=C< bonds. The most intense frequency is obtained at 1963 cm^{-1} for carbonyl –C=O stretching. We found that OL3-B(L) gives similar results

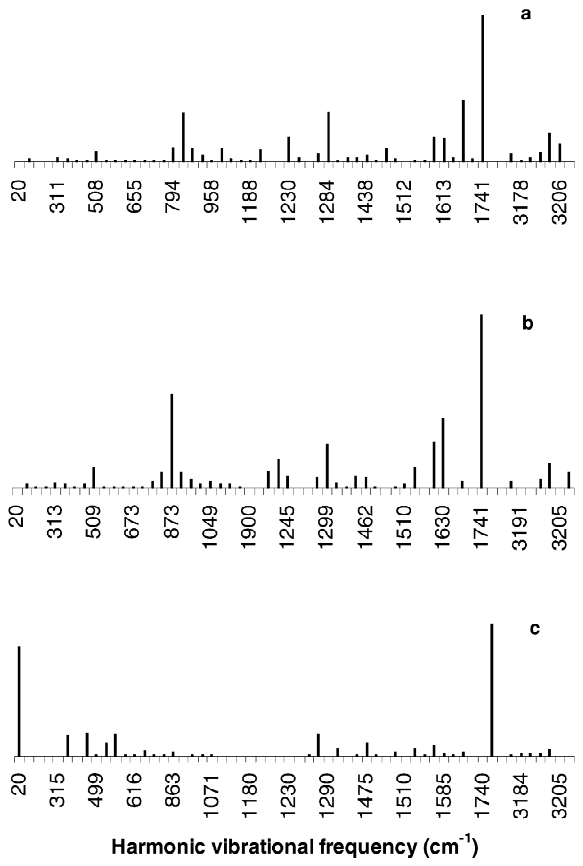

Fig. 4. Predicted IR spectra for the semiquinone–zigzag surface complex using different computational levels. (a) B3LYP/6-31G(d); (b) OL3-B(L); (c) OL2-BA(L).

Fig. 5. Predicted IR spectra for the carbonyl–armchair surface complex using different computational levels. (a) B3LYP/6-31G(d); (b) OL3-B(L); (c) OL2-BA(L).

for this complex. In particular, frequencies in Fig. 5b centered at 1963 cm^{-1} correspond to carbonyl –C=O stretching. Frequencies over 3000 cm^{-1} are the >C–H stretching and those between 1400 and 1600 cm^{-1} are due to the >C=C< bond. The intensity patterns and the frequency values resemble those obtained at the B3LYP/6-31G(d) level. Fig. 5c shows the predicted IR spectrum obtained at the OL2-BA(L) level of theory. Frequencies at 1942 and 1958 cm^{-1} are due to –C=O stretching. The frequency values are close to the carbonyl –C=O stretching obtained at B3LYP/6-31G(d). However, the highest intensity in the OL2-BA(L) spectrum was obtained at 2455 cm^{-1}, which is assigned to the >C=C< stretching mode. The general pattern of the OL2-BA(L) spectrum does not resemble the spectrum obtained at the B3LYP/6-31G(d) level.

Finally, we examine the computational cost for the ONIOM methods. Table 7 lists the average time per optimization cycle (hour/cycle) of the carbonaceous models and their corresponding surface carbon–oxygen complexes. These results are relative to the least expensive method, i.e., the OL2-BA(R) method. It was found that the computational cost increases in the order OL2-BA(R) ≅ OL2-BA(L)<OL2-BH(L)<OL3-B(L)<B3LYP/6-31G(d). The computational costs of OL2-BA(R) and OL2-BA(L) were the less time-demanding, while our reference point, the B3LYP/6-31G(d) level, is about 12 times more expensive in some cases. The OL3-B(L) model is about a factor of two times faster than the B3LYP/6-31G(d) level.

Besides the computational time demand, we found that any attempt to partition the system into subsystems and treat them at different levels of theory would lead to large errors. This is because such partitions would disrupt the electron delocalization of the π-bond network. However, we found that it is possible to treat different regions with different basis sets and still maintain a reasonable level of accuracy. Given its performance on the geometry, interaction energy and IR spectra, the OL3-B(L) method can be used in future studies of adsorption or chemical processes on large carbonaceous surfaces.

Table 7
Relative time per cycle during the optimization of the armchair and zigzag models at different levels of theory[a]

Level of theory	Armchair			Zigzag		
	Carbon model	Semiquinone	Carbonyl	Carbon model	Semiquinone	Carbonyl
OL2-BA(R)	1.0	1.0	1.0	1.0	1.0	1.0
OL2-BA(L)	1.2	1.0	0.9	1.0	1.0	1.0
OL2-BH(L)	1.7	6.4	1.6	2.0	1.7	2.5
OL3-B(L)	3.4	6.0	4.4	5.8	2.5	3.6
B3LYP/6-31G(d)	9.1	10.2	7.8	12.6	3.9	10.6

[a] All values are relative to the O-BA(R) level.

4. Conclusions

We have performed a systematic study of the accuracy and efficiency of different quantum chemistry methods for studying the chemistry of carbonaceous materials. In particular, these methods were evaluated for the prediction of geometrical parameters, interaction energies and IR spectra of surface complexes. We found that the HF method is inadequate to represent the interaction energy of carbon monoxide and atomic oxygen with carbonaceous surfaces due to the lack of electron correlation and the large spin contamination in the ground state wavefunction. Different ONIOM methods with different partition schemes for dividing the whole system into subsystems were also investigated. We found that any attempt to partition the system into subsystems and treat them at different levels of theory would lead to large errors. This is because the carbonaceous surfaces are highly aromatic. Such a partition would disrupt the delocalization of the π-bond network. However, we found that it is possible to treat different regions with different basis sets and still maintain a reasonable level of accuracy. This, in fact, gives a noticeable decrease in the computational cost and thus the approach is recommended for future studies of adsorption on large carbonaceous surfaces.

Acknowledgements

F. Mondragón and A. Montoya wish to thank Colciencias and the University of Antioquia for financial support of project No. 1115-05-10853. T.N. Truong acknowledges financial support from NSF. A. Montoya wishes to thank the seed grant given by the University of Utah. We also thank the Utah Center for High Performance Computing for computer time support.

References

[1] Montoya A, Truong TN, Sarofim AF. Application of density functional theory to the study of the reaction of NO with char-bound nitrogen during combustion. J Phys Chem A 2000;104(36):8410–8.
[2] Kyotani T, Tomita A. Analysis of the reaction of carbon with NO/N_2O using ab initio molecular orbital theory. J Phys Chem B 1999;103(17):3434–41.
[3] Chen N, Yang RT. Ab initio molecular orbital study of the unified mechanism and pathways for gas–carbon reactions. J Phys Chem A 1998;102(31):6348–56.
[4] Chen SG, Yang RT. The active surface species in alkali-catalyzed carbon gasification: phenolate (C–O–M) groups vs. clusters (particles). J Catal 1993;141(1):102–13.
[5] Iijima S, Ajayan PM, Ichihashi T. Growth model for carbon nanotubes. Phys Rev Lett 1992;69(21):3100–3.
[6] Maiti A, Brabec CJ, Roland C, Bernholc J. Theory of carbon nanotube growth. Phys Rev B 1995;52(20):14850–8.
[7] Bernholc J, Brabec C, Nardelli MB, Maiti A, Roland C, Yakobson BI. Theory of growth and mechanical properties of nanotubes. Appl Phys A 1998;67(1):39–46.
[8] Bengu E, Marks LD. Single-walled BN nanostructures. Phys Rev Lett 2001;86(11):2385–7.
[9] Radovic LR, Walker Jr. PL, Jenkins RG. Importance of carbon active sites in the gasification of coal chars. Fuel 1983;62(7):849–56.
[10] McEnaney B. Active sites in relation to gasification of coal char. In: Lahaye J, Ehrburger P, editors, Fundamental issues in the control of carbon gasification reactivity, NATO ASI, vol. 192, Dordrecht: Kluwer, 1991, pp. 165–203.
[11] Berkowitz N. The chemistry of coal. New York: Elsevier, 1985.
[12] Marzec A, Czajkowska S, Moszynski J. Electrical resistivity of carbonized coals. Energy Fuels 1994;8(6):1296–303.
[13] Oberlin A. Carbonization and graphitization. Carbon 1984;22(6):521–41.
[14] Ajayan PM, Ichihashi T, Iijima S. Distribution of pentagons and shapes in carbon nano-tubes and nano-particles. Chem Phys Lett 1993;202(5):384–8.
[15] Perry ST, Hambly EM, Fletcher TH, Solum MS, Pugmire RJ. Solid-state ^{13}C NMR characterization of matched tars and chars from rapid coal devolatilization. Proc Combust Inst 2000;28:2313–9.
[16] Chen N, Yang RT. Ab initio molecular orbital calculation on graphite: selection of molecular system and model chemistry. Carbon 1998;36(7/8):1061–70.
[17] Moriguchi K, Munetoh S, Abe M, Yonemura M, Kamei K, Shintani A et al. Nano-tube-like surface structure in graphite particles and its formation mechanism: a role in anodes of

lithium-ion secondary batteries. J Appl Phys 2000;88(11):6369–77.
[18] Svensson M, Humbel S, Froese RDJ, Matsubara T, Sieber S, Morokuma K. ONIOM: a multi-layered integrated MO+MM method for geometry optimizations and single point energy predictions. A test for Diels–Alder reactions and $Pt(P(t\text{-}Bu)_3)_2+H_2$ oxidative addition. J Phys Chem 1996;100(50):19357–63.
[19] Dapprich S, Komiromi I, Byun KS, Morokuma K, Frisch MJ. A new ONIOM implementation in Gaussian98. Part I. The calculation of energies, gradients, vibrational frequencies and electric field derivatives. Theochem 1999;461/462:1–21.
[20] Froese RDJ, Morokuma K. IMOMO-G2MS approaches to accurate calculations of bond dissociation energies of large molecules. J Phys Chem A 1999;103(23):4580–6.
[21] Froese RDJ, Morokuma K. Accurate calculations of bond-breaking energies in C60 using the three-layered ONIOM method. Chem Phys Lett 1999;305(5/6):419–24.
[22] Montoya A, Truong T-TT, Mondragon F, Truong TN. CO desorption from oxygen species on carbonaceous surface: 1. Effects of the local structure of the active site and the surface coverage. J Phys Chem A 2001;105(27):6757–64.
[23] Becke AD. Density-functional thermochemistry. III. The role of exact exchange. J Chem Phys 1993;98(7):5648–52.
[24] Easton RE, Giesen DJ, Welch A, Cramer CJ, Truhlar DG. The MIDI! basis set for quantum mechanical calculations of molecular geometries and partial charges. Theor Chim Acta 1996;93(5):281–301.
[25] Marzec A. New structural concept for carbonized coals. Energy Fuels 1997;11(4):837–42.
[26] Frisch MJ, Trucks GW, Schlegel HB, Scuseria GE, Robb MA, Cheeseman JR et al. Gaussian 98, rev. A.9. Pittsburgh, PA: Gaussian, Inc, 1998.
[27] CRC handbook of chemistry and physics. 81st ed. Cleveland, OH: CRC Press, 2000:9–19.
[28] Montoya A, Truong TN, Sarofim AF. Spin contamination in Hartree–Fock and density functional theory wavefunctions in modeling of adsorption on graphite. J Phys Chem A 2000;104(26):6108–10.